

# Lithium Ethylene Dicarboxate Identified as the Primary Product of Chemical and Electrochemical Reduction of EC in 1.2 M LiPF<sub>6</sub>/EC:EMC Electrolyte

Guorong V. Zhuang,<sup>\*,†</sup> Kang Xu,<sup>‡</sup> Hui Yang,<sup>§</sup> T. Richard Jow,<sup>‡</sup> and Philip N. Ross, Jr.<sup>†</sup>

Materials Sciences and Environmental Energy Technologies Division, Lawrence Berkeley National Laboratory, University of California, Berkeley, California 94720, and U.S. Army Research Laboratory, Adelphi, Maryland 20783

Received: May 11, 2005; In Final Form: July 19, 2005

Lithium ethylene dicarbonate ((CH<sub>2</sub>OCO<sub>2</sub>Li)<sub>2</sub>) was chemically synthesized and its Fourier transform infrared (FTIR) spectrum was obtained and compared with that of surface films formed on Ni after cyclic voltammetry (CV) in 1.2 M lithium hexafluorophosphate (LiPF<sub>6</sub>)/ethylene carbonate (EC):ethyl methyl carbonate (EMC) (3:7, w/w) electrolyte and on metallic lithium cleaved in-situ in the same electrolyte. By comparison of IR experimental spectra with that of the synthesized compound, we established that the title compound is the predominant surface species in both instances. Detailed analysis of the IR spectrum utilizing quantum chemical (Hartree–Fock) calculations indicates that intermolecular association through O···Li···O interactions is very important in this compound. It is likely that the title compound in the passivation layer has a highly associated structure, but the exact intermolecular conformation could not be established on the basis of analysis of the IR spectrum.

## I. Introduction

Lithium ethylene dicarbonate ((CH<sub>2</sub>OCO<sub>2</sub>Li)<sub>2</sub>) has been proposed by Aurbach et al.<sup>1–5</sup> as one of the reduction products of ethylene carbonate (EC) on noble metals and lithium electrodes. The proposed single-electron reduction path is as follows:



The above path was extended later by Aurbach and co-workers to the electrochemical reduction process of EC on carbonaceous anode surfaces and eventually led to the general belief inherited by Li ion battery industry and research community that this dicarbonate plays a major role in constituting the protective film on the carbonaceous anode (solid electrolyte interphase, or SEI) so that reversible lithium ion chemistry could occur. The details have been summarized in a comprehensive review article by Xu.<sup>6</sup> However, due to the unusual sensitivity of the title compounds toward ambient moisture, there was never an affirmative identification that could directly link the title compound to the species detected spectroscopically on electrode surfaces. The closest identification of this compound comes from the FTIR spectrum obtained from the electrolysis product of EC in tetrahydrofuran (THF) + 0.5 M tetrabutylammonium perchlorate (TBAP) on a gold electrode, which was isolated from electrolyzed solutions in the form of precipitation.<sup>2</sup> The obtained product is speculated to be (CH<sub>2</sub>OCO<sub>2</sub>Li)<sub>2</sub>, which would be consistent with an EC single-electron reduction mechanism shown in eq 1. The <sup>1</sup>H nuclear magnetic resonance (NMR) collected from the decomposition of the electrolysis

product in deuterated water (D<sub>2</sub>O) seemed to support this speculation. Nevertheless, the identity of this key species of SEI remains elusive mainly for two reasons: (a) the hitherto absence of true reference compound and its reference spectrum; (b) difficulties in obtaining high-quality FTIR spectra on the electrode surface after electrochemical processes, thus allowing unambiguous identification of such species. Given the critical role of the title compound and other alkyl carbonates in the surface chemistry of Li-ion battery technology, the in-depth understanding of their formation and physical/thermal properties would be of significant value to this Li-ion battery research field. Thus, collaboration between Lawrence Berkeley National Laboratory (LBNL) and the U. S. Army Research Laboratory (ARL) was established, which combined the expertise in chemical synthesis, electrochemistry, spectroscopic characterization, and computation modeling. The present paper presents some of the results generated by this collaborative effort.

In this work, lithium ethylene dicarbonate was chemically synthesized and its FTIR spectrum was obtained and compared with that of surface films formed on Ni after cyclic voltammetry in 1.2 M LiPF<sub>6</sub>/EC:EMC (3:7, w/w; EMC = ethyl methyl carbonate) electrolyte. The chemical synthesized compound was also reported recently by Tarascon et al. via a different synthesis route.<sup>7</sup> This direct comparison allows us to identify (CH<sub>2</sub>OCO<sub>2</sub>Li)<sub>2</sub> as the predominant reduction product, in addition to electrolyte residues, in support of EC reduction path (1) on inert metal electrode. These results also provide fingerprints of lithium ethylene dicarbonate in experimental FTIR spectroscopy, which would serve as a reference for SEI components identification in future studies, as well as experimental validation of theoretical approaches.

## II. Experimental Section

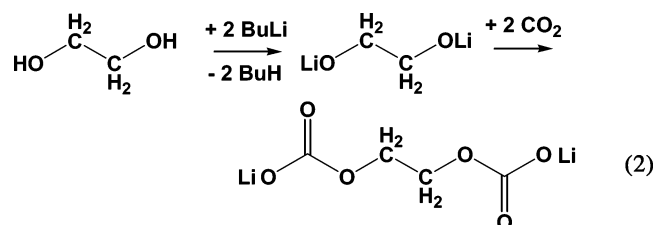
(LiOCO<sub>2</sub>CH<sub>2</sub>)<sub>2</sub> was synthesized in ARL by the following route:

\* Corresponding author. E-mail: GVZhuang@lbl.gov.

<sup>†</sup> Materials Sciences Division, Lawrence Berkeley National Laboratory, University of California, Berkeley.

<sup>‡</sup> U.S. Army Research Laboratory.

<sup>§</sup> Environmental Energy Technologies Division, Lawrence Berkeley National Laboratory, University of California, Berkeley.



All the reaction and purification procedures were carried out in a dry room with dew points below  $-85^\circ\text{C}$ . A flask equipped with reflux condenser was charged with 30 mL of 2.5 M butyllithium (LiBu) solution in *n*-hexane with an additional 200 mL of anhydrous ether used as diluent solvent. A total of 2.3 g of ethylene glycol was then added dropwise into the LiBu solution with vehement stirring. The mixture temperature was maintained below  $30^\circ\text{C}$  by adjusting the addition rate. After the addition, the reaction mixture became a milky suspension of lithium ethylene dialkoxide ( $\text{LiOCH}_2\text{CH}_2\text{OLi}$ ), into which the analytic grade of carbon dioxide ( $\text{CO}_2$ ) was introduced. An immediate change was observed as the white flake crystals formed as precipitation. After introduction of an excess amount of  $\text{CO}_2$ , the crystalline product was repeatedly washed with dried acetonitrile following filtration. The sample was further dried under vacuum at ambient temperature overnight. The dried sample was then sealed in an argon (Ar) glovebox and shipped to LBNL.

Electrochemical measurements were carried out in an Ar-filled glovebox, with  $\text{O}_2$  content  $< 1$  ppm and  $\text{H}_2\text{O}$  content  $< 2$  ppm, using a three-electrode glass cell. A high-temperature annealed and polished nickel (Ni) foil (99.999%,  $0.95\text{ cm}^2$ ) was used as a working electrode, and lithium was used as both counter and reference electrodes. The electrolyte was 1.2 M  $\text{LiPF}_6/\text{EC}:\text{EMC}$  (3:7, w/w). The electrochemical cell was sealed to prevent evaporation of the volatile electrolyte component, EMC, during the experiments. All cyclic voltammetry (CV) measurements were performed at ambient temperature with a computer-controlled Gamry PCI 4/300 potentiostat. Following voltammetry, which included lithium deposition, the Ni electrode was removed after the final sweep in the positive direction to 2.5 V, i.e., after the anodic stripping of any deposited lithium. The Ni electrode was placed in a vacuum transfer vessel in the glovebox, and the sealed transfer vessel was taken to the FTIR spectrometer. The sample chamber of the spectrometer has a helium gas-purged enclosure that permits sample mounting without air exposure.

To study chemical reduction, on metallic lithium, of electrolyte used in electrochemical reduction, a lithium (Li) foil (99.9%, Aldrich) was cleaved in situ and left in the electrolyte for a few minutes in an Ar-filled glovebox. The sample transfer and measurement followed the identical procedures as that of Ni electrode after CV.

As a control sample for the IR spectrum of residual electrolyte, a gold foil was simply stored in the same electrolyte for several days in the glovebox and then removed and analyzed in the same manner as the Ni electrode after CV. All the IR spectra were acquired in the attenuated total reflection (ATR) mode at a  $4\text{ cm}^{-1}$  resolution and summed over 512 scans. Details of our ATR mode for FTIR analysis have been reported in earlier publications.<sup>8,9</sup>

### III. Computation

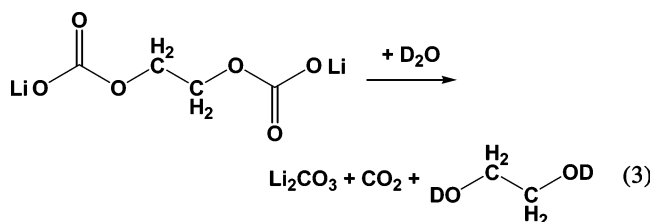
We performed ab initio quantum chemical calculations using Gaussian 98<sup>10</sup> at the Hartree–Fock (HF) theory level with a 6-31+G(d,p) basis set. The molecular structure was optimized

first prior to frequency calculations at the same theory level and with the basis set. The systematic error in calculated vibrational frequencies at the HF level was corrected by using an empirical scaling factor of 0.8929.<sup>11</sup>

### IV. Results and Discussions

#### Structural Identification of Synthetic $(\text{CH}_2\text{OCO}_2\text{Li})_2$ .

Approximately 20 mg of the synthesized title compound was mixed with 3 mL of acetone- $d_6$  in an NMR tube. Since this dicarbonate salt is barely soluble, a suspension was obtained.  $^1\text{H}$  and  $^{13}\text{C}$  NMR spectra were collected from this suspension with a 400 MHz Oxford spectrometer. The spectra (Figure 1A) showed a  $^1\text{H}$  signal at 3.53 ppm (singlet) as well as  $^{13}\text{C}$  signals at 62.96 ppm (singlet, for C2) and 157 ppm (singlet, for C1). Due to the trace presence of the salt in solution and the low abundance of  $^{13}\text{C}$  nuclei, the background noise arising from the deuterated solvent remains highly interfering, especially so for the  $\text{sp}^2$ -hybridized carbonyl carbon (C1). To confirm the existence of the carbonyl functionalities—so that the structure of  $(\text{CH}_2\text{OCO}_2\text{Li})_2$  could be affirmed beyond any doubt—we deliberately decomposed it with  $\text{D}_2\text{O}$  and carried out further NMR measurements (Figure 1B) on the resultant  $\text{D}_2\text{O}$  solution. It was found that the  $^1\text{H}$  signal was shifted to 3.58 ppm, while a conspicuous  $^{13}\text{C}$  peak was detected at 160 ppm, indicating that deuterated ethylene glycol and lithium carbonate ( $\text{Li}_2\text{CO}_3$ ) were formed as a result of deuteriolysis:



Therefore, the crystalline product obtained via synthetic path (2) is in fact the desired compound  $(\text{CH}_2\text{OCO}_2\text{Li})_2$ .

The FTIR spectrum of the synthesized  $(\text{CH}_2\text{OCO}_2\text{Li})_2$  is shown in Figure 2. To aid in interpretation of the IR spectrum, we calculated vibrational frequencies of the compound by ab initio quantum chemical calculation. The optimized structures of the  $(\text{CH}_2\text{OCO}_2\text{Li})_2$  single molecule and its dimer are shown in Figure 3A and B, respectively. The calculated normal mode vibrational frequencies and their comparison to experimental frequencies are tabulated in Table 1, as well as characteristic FTIR spectral feature assignments to  $(\text{CH}_2\text{OCO}_2\text{Li})_2$ .

The  $\text{O}(1)\text{C}(1)\text{O}(1)\text{O}(2)$  symmetric stretching mode, coupled with the  $\text{C}(2)\text{H}(1)_2$  twisting mode, is predicted to be at  $1427\text{ cm}^{-1}$  by quantum chemical calculation but is observed at  $1402\text{ cm}^{-1}$  experimentally. The combination of  $\text{C}(1)\text{O}(2)\text{C}(2)$  asymmetric and  $\text{O}(1)\text{C}(1)\text{O}(1)$  symmetric vibrational modes gives rise to a medium-intensity peak at  $1062\text{ cm}^{-1}$ , shifting significantly to lower wavenumber than the theoretically predicted position as well. The peak at  $825\text{ cm}^{-1}$  is characteristic of the semi-carbonate group  $\text{O}(1)\text{C}(1)\text{O}(1)\text{O}(2)$  out-of-plane bending mode, while the weak peak at  $726\text{ cm}^{-1}$  is attributed to coupling of  $\text{O}(1)\text{C}(1)\text{O}(1)$  and  $\text{C}(1)\text{O}(2)\text{C}(2)$  deformation modes. The strongest peak at  $1663\text{ cm}^{-1}$  is characteristic of the asymmetry stretching mode of the  $\text{O}(1)\text{C}(1)\text{O}(1)$  resonance, with a bond order of 1.5; i.e., the two oxygens O(1) in this molecule are chemically equivalent. However, the  $\text{O}(1)\text{C}(1)\text{O}(1)$  resonance, a very reliable group frequency, compares unsatisfactorily with the calculated frequency of  $1582\text{ cm}^{-1}$  in single molecule  $(\text{CH}_2\text{OCO}_2\text{Li})_2$ . Although many of the experimental spectral features

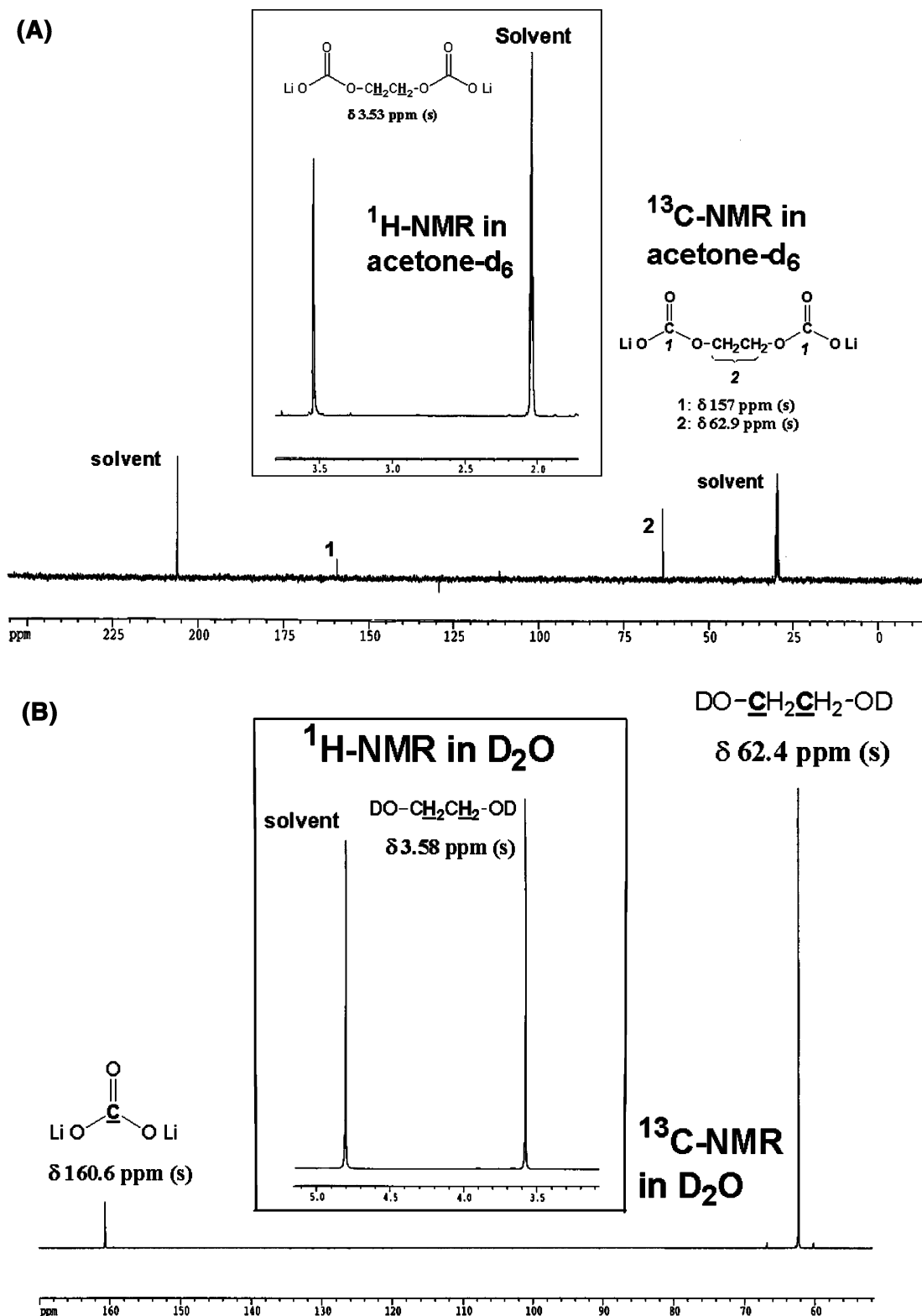


**Figure 1.** (A) <sup>1</sup>H and <sup>13</sup>C NMR of lithium ethylene dicarbonate in acetone-d<sub>6</sub>; (B) <sup>1</sup>H and <sup>13</sup>C NMR of lithium ethylene dicarbonate decomposition products in D<sub>2</sub>O.

could be assigned with the aid of quantum chemical calculations based on the single molecule model (Figure 3A) at HF level, it is evident that theoretical calculation for the single molecule does not reproduce the most reliable group frequencies with the expected accuracy nor capture the peak splitting at ca. 1400 and 1310 cm<sup>-1</sup>, and completely missed the experimental peaks at 1115 and 1006 cm<sup>-1</sup>. Calculation at a much higher theory level, B3PW91/6-31G(d),<sup>12</sup> on the (CH<sub>2</sub>OCO<sub>2</sub>Li)<sub>2</sub> molecule did not improve the agreement with experiment, implying that it is

the model rather than the theory level used that fails to reproduce these experimentally observed vibrational modes. These extra features are most likely due to strong intermolecular interactions from either dimer formation or other solid-state effects, e.g. coupling, neglected in the single-molecule calculation.

To explore the effect of intermolecular interactions on vibrational modes, the dimer structure proposed by Wang and Balbuena<sup>12</sup> was used and was optimized at the same theory level as the (CH<sub>2</sub>OCO<sub>2</sub>Li)<sub>2</sub> single molecule calculation, i.e., at the

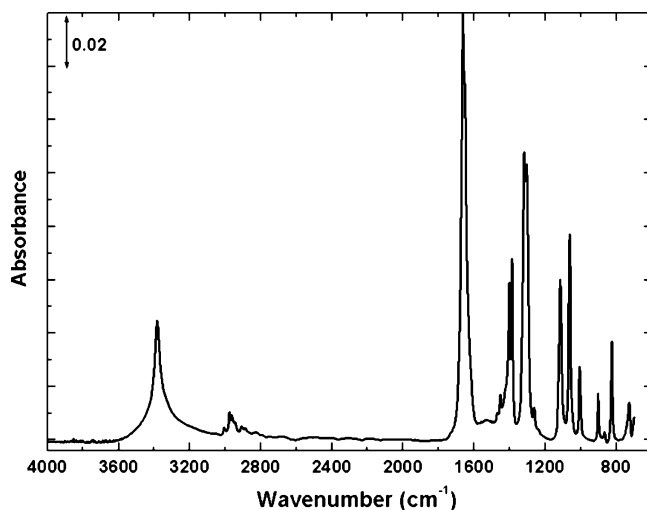
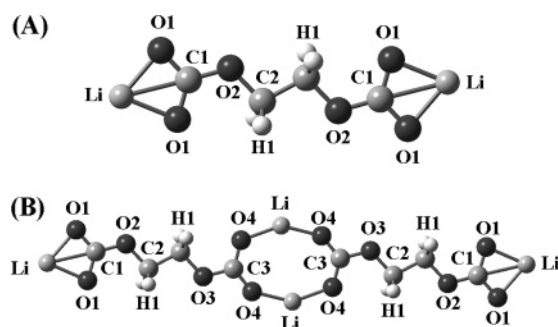
**TABLE 1: Comparison of Experimental and Calculated Vibrational Frequencies of Lithium Ethylene Dicarboxylate Single Molecule and Dimer**

experimental frequency (cm <sup>-1</sup> )	monomer calcd frequency (cm <sup>-1</sup> )	dimer calcd frequency (cm <sup>-1</sup> )	assignment
2975	2962	2960	C(2)H(1) <sub>2</sub> asymmetric stretching
2961	2903	2902	C(2)H(1) <sub>2</sub> asymmetric stretching
2943		2898	
1663		1651	O(4)C(3)O(4) asymmetric stretching
	1582	1583	O(1)C(1)O(1) asymmetric stretching
1452	1483	1484	C(2)H(1) <sub>2</sub> deformation (scissoring)
		1457	C(2)H(1) <sub>2</sub> deformation (scissoring) + C(1)O(2)C(2) & C(3)O(3)C(2)
1402	1427	1412	O(1)C(1)O(1)O(2) asymmetric stretching + C(2)H(1) <sub>2</sub> twisting
1385		1389	O(3)C(3)O(4)O(3) asymmetric stretching + C(2)H(1) <sub>2</sub> twisting
1318, 1302	1311	1307	C(2)H(1) <sub>2</sub> wagging (unreliable group frequency)
1115	—	1151	C(3)O(3)C(2) asymmetric stretching
1061	1137	1131	C(1)O(2)C(2) asymmetric + O(1)C(1)O(1) symmetric stretching
1006	—	965	O(4)C(3)O(4)O(3) symmetric stretching + C(1)O(2)C(2) symmetric stretching
825	840	840	CO <sub>3</sub> out of plane bending + C(2)H(1) <sub>2</sub> out of plane rocking (twisting)
726	740	746	O(1)C(1)O(1) deformation + C(1)O(2)C(2) deformation

HF/ 6-31+G(d,p) level. The vibrational calculation on the optimized dimer structure (Figure 3B) is presented in Table 1. In the dimer structure, the semi-carbonate groups, i.e., O(3)C(3)O(4)O(4), involved in dimerization have a different chemical environment than their counterpart, O(2)C(1)O(1)O(1). Such a unique environment gives rise to 1115 and 1006 cm<sup>-1</sup>, as well as peak splitting at ca. 1400 cm<sup>-1</sup>. The most interesting aspect revealed by the dimer model calculation is the difference in vibrational frequencies of the O(1)C(1)O(1) and O(4)C(3)O(4) asymmetric stretching mode, from 1583 cm<sup>-1</sup> for the single molecule to 1651 cm<sup>-1</sup> in the dimer. The excellent agreement of the frequency calculated for the dimer model and the

experimental vibrational mode at 1663 cm<sup>-1</sup> strongly suggests that the (CH<sub>2</sub>CH<sub>2</sub>OCO<sub>2</sub>Li)<sub>2</sub> molecules in the solid state are associated with each other via O...Li...O interactions.

**Analysis of Surface Species Formed after Lithium Deposition on Ni.** The CV obtained in 1.2 M LiPF<sub>6</sub>/EC:EMC (3:7, w/w) electrolyte on the Ni electrode is shown in Figure 4A. The potential was swept from an open circuit voltage (OCV) of 2.9 to 0.5 V, followed by reverse scan from 0.5 to 2.5 V vs Li/Li<sup>+</sup>, at a scan rate of 1 mV/s. A pronounced cathodic peak observed in the first cycle, presumably due to the electrolyte solvent reduction, was not observed on subsequent cycles, indicating the Ni surface became passive to electrolyte reduction in this potential range. The total charge under the reduction peak was ca. 0.01 C/cm<sup>2</sup>. The chemical nature of the passivation layer was revealed by an FTIR spectrum (Figure 5, spectrum c)

**Figure 2.** FTIR spectrum of synthetic lithium ethylene dicarbonate.



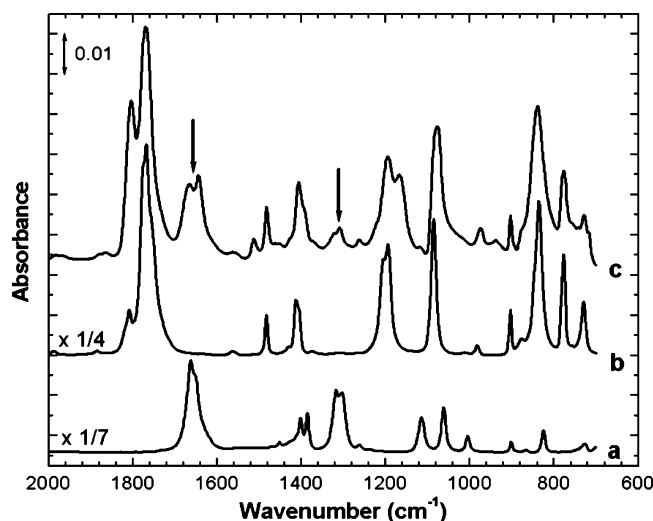


**Figure 5.** FTIR spectra of (a) synthetic lithium ethylene dicarbonate; (b) EC solvate; and (c) the surface of the Ni electrode cycled between 0.5 and 2.5 V vs  $\text{Li}/\text{Li}^+$  (see Figure 4A).

obtained on the Ni electrode after the cyclic voltammetry shown. Although the Ni electrode was still covered with  $\text{EC}:\text{LiPF}_6$  solvate, two unique features at 1660 and 1310  $\text{cm}^{-1}$  (marked by arrows above spectrum c) appeared in the spectral region where the residual electrolyte has no vibrational modes (see spectrum b in Figure 5). Interestingly, those new peaks are two of the characteristic vibrational modes in the synthesized  $(\text{CH}_2\text{OCO}_2\text{Li})_2$  (spectrum a in Figure 5). However, the passive layer was not sufficiently adherent to the Ni surface to survive rinsing with dimethyl carbonate (DMC); i.e., all attempts to rinse just the residual electrolyte from the electrode resulted in removal of the passive film as well.

A more adherent and robust reduction product was observed on the Ni electrode after cycling through the potential region, which included lithium deposition and stripping. The first sweep is shown in Figure 4B. The CV has a classic appearance with a “nucleation loop” characteristic of deposition by a nucleation and growth mechanism<sup>13</sup> and is qualitatively very similar to the first sweep on a Ni microdisk electrode in 1 M  $\text{LiAsF}_6/\text{propylene carbonate}$  (PC) electrolyte reported by Pletcher et al.<sup>14</sup> The cycling efficiency, defined as the ratio of anodic to cathodic charge in a single cycle, varied with the number of cycles, as shown in the insert. Lithium cycling efficiencies of 50–75% are also very similar to those reported by Pletcher et al.<sup>14</sup> and more recently by the Mitsubishi group.<sup>15</sup> The electrode was removed from the cell after the ninth sweep to 2.5 V and the surface analyzed by FTIR. After elimination of most of the residual electrolyte by controlled rinsing with DMC, the remaining reduction product clearly evolved from the spectral features denoted by the arrows in the original (no rinsing) spectrum from the electrode cycled only to +0.5 V, i.e., without lithium deposition. This was strong, but not definitive evidence, that the reduction product formed below +0.5 V accompanying lithium deposition is the same as that formed initially in the +0.5 to +2.5 V region. As pointed out by Pletcher et al.<sup>14</sup> previously, the initial electrochemical processes in this potential region include the reduction of water (and possibly other impurities) in the electrolyte, as in fact we can see that in the spectra, as discussed below. As clearly shown in Figure 6, the spectrum b from the Ni surface has *all* the vibrational modes present in that of the synthesized lithium ethylene dicarbonate, both in vibrational frequencies and relative intensity between 2000 and 700  $\text{cm}^{-1}$ . Several weak peaks, not present in the lithium ethylene dicarbonate spectrum, could be readily at-

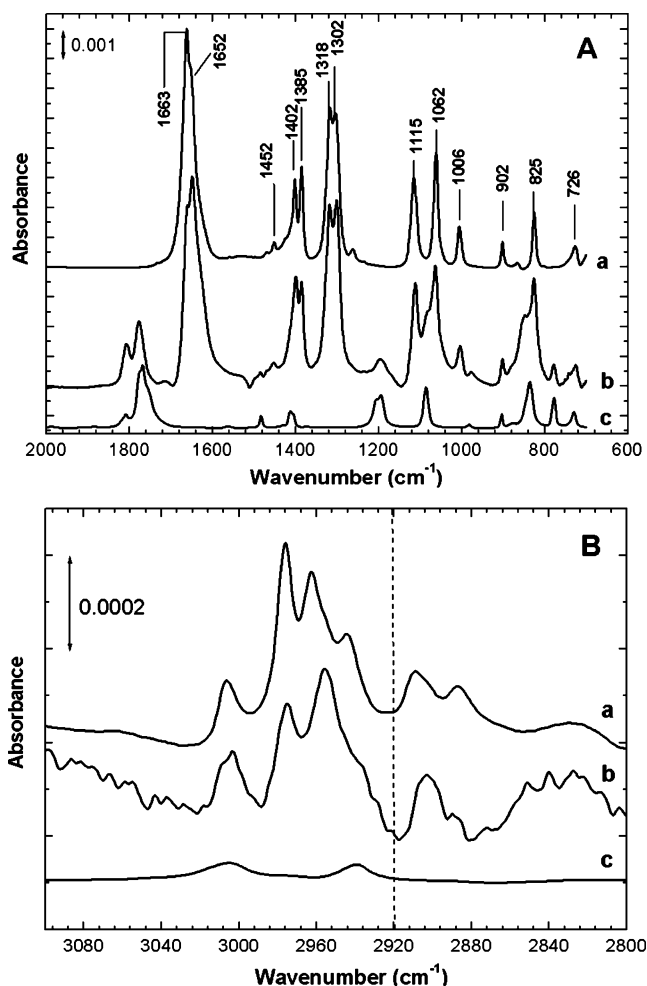


**Figure 6.** FTIR spectra of (a) synthetic lithium ethylene dicarbonate; (b) surface species on the Ni electrode after Li deposition cycling between  $-0.5$  and  $+2.5$  V (see Figure 4B); (c)  $\text{EC}:\text{LiPF}_6$  solvate.

tributed to electrolyte residue remaining on the surface (see Figure 6, spectrum c). Virtually *all* of the spectral features on the Ni electrode after lithium cycling could be accounted for by superposition of lithium ethylene dicarbonate and residual electrolyte ( $\text{EC}:\text{LiPF}_6$  solvate).

It is very difficult even to estimate the thickness of the lithium ethylene dicarbonate layer on the Ni surface after this experiment on the basis of the absolute intensities of the IR bands. We can, however, estimate this thickness from the total charge of ca. 0.01  $\text{C}/\text{cm}^2$  under the reduction peak in Figure 4A, assuming all the charge goes to reduction of EC to lithium ethylene dicarbonate. Using 4  $\text{e}^-/\text{dimer}$ , there would be ca.  $1.56 \times 10^{16}$  dimers/ $\text{cm}^2$ . Assuming the lithium ethylene dicarbonate dimer structures are cylinders being 20 Å in length and 3 Å in diameter and a monolayer is formed by laying these cylinders end-to-end and side-to-side, there are  $1.67 \times 10^{14}$  (dimers/ $\text{cm}^2$ )/monolayer. The thickness therefore is about 100 monolayers or about 300 Å (30 nm), consistent with 10–100 nm as the order of magnitude of passive layer thickness suggested by several different studies.<sup>16,17</sup>

As shown by the spectra in Figure 7, the purely chemical reaction between an in-situ cleaved surface of metallic lithium and this same electrolyte produced virtually an identical surface layer on the lithium as on the Ni after lithium deposition and dissolution. Note that these spectra also include the region around 3600  $\text{cm}^{-1}$ , the O–H stretching frequency region, and the features in this region in the spectra of the lithium and Ni surfaces as mentioned above can be attributed to  $\text{LiOH} \cdot n\text{H}_2\text{O}$

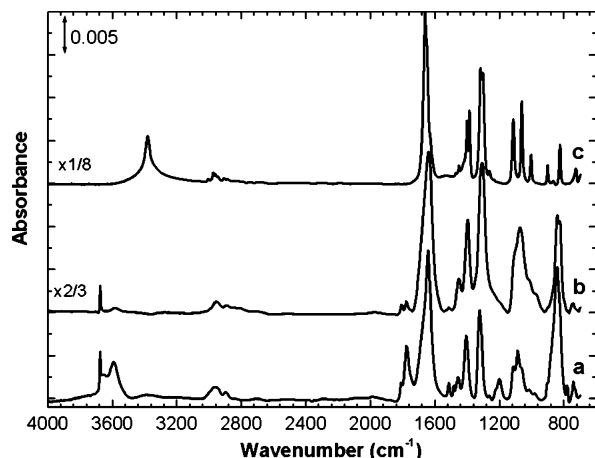


**Figure 7.** FTIR spectra of (a) the surface film formed on freshly cleaved metallic Li in 1.2 M LiPF<sub>6</sub>/EC:EMC (3:7); (b) the Ni electrode after a total of nine cycles of Li deposition and dissolution; (c) synthetic lithium ethylene dicarbonate.

from water reduction (the feature at 3300 cm<sup>-1</sup> in the synthesized (CH<sub>2</sub>OCO<sub>2</sub>Li)<sub>2</sub> spectrum is from residual (ethylene glycol)).

It is informative to discuss the implications of our experimental findings in the context of theoretical studies of the mechanism of electrochemical reduction of EC. High-level density functional theory (DFT) calculation considered five different paths for termination of the one-electron EC radical anion,<sup>18</sup> identifying two barrierless dimerization pathways, resulting in either lithium butylene dicarbonate (CH<sub>2</sub>CH<sub>2</sub>OCO<sub>2</sub>Li)<sub>2</sub> or lithium ethylene dicarbonate (CH<sub>2</sub>OCO<sub>2</sub>Li)<sub>2</sub>. These two were the energetically most favorable pathways of the five considered. In our synthesis of the latter compound, we could distinguish the absence of the former as alkyl (-CH<sub>2</sub>-) carbon and ethoxy (-CH<sub>2</sub>O-) carbons are easily differentiated by their chemical shifts and characteristic splitting patterns in NMR. In both <sup>1</sup>H and <sup>13</sup>C NMR of the synthesis product in acetone-*d*<sub>6</sub> or D<sub>2</sub>O, only one type of sp<sup>3</sup> carbon, corresponding to the carbon in ethoxy, was found. In the case of IR spectroscopy, the spectral region between 3100 and 2800 cm<sup>-1</sup> is the region where the two carbonates could be distinguished. Of particular importance is the absence of characteristic ethylene (-CH<sub>2</sub>-) group frequencies at 2920 and 2850 cm<sup>-1</sup> in spectrum b, lower panel, Figure 6. Such vibrational frequencies would be found if (CH<sub>2</sub>CH<sub>2</sub>OCO<sub>2</sub>Li)<sub>2</sub> instead of (CH<sub>2</sub>OCO<sub>2</sub>Li)<sub>2</sub> is one of the main reduction products of the surface SEI layer components. However, if (CH<sub>2</sub>CH<sub>2</sub>OCO<sub>2</sub>Li)<sub>2</sub> has high solubility in electrolyte, it will not be resolved on the electrode surface by our measurements.

Another interesting implication of our result is that there was no evidence of the involvement of the cosolvent EMC in the formation of the surface layers. As pointed out so elegantly in the DFT calculations by Wang et al.,<sup>18</sup> lithium ion solvation plays an important role in lowering the energy barrier for electron transfer to form the radical anion; i.e., the EC molecules solvating lithium ions are selectively reduced. Due to much higher dielectric constant (ε = 90) of EC than that of its cosolvent EMC (ε = 3),<sup>6</sup> EC would be expected to be the primary molecule in the inner solvation sheath of lithium ion in an EC:EMC cosolvent.<sup>19</sup> Recent studies on various Li-ion battery electrolytes by Arakawa et al.<sup>20</sup> using electrospray ionization mass spectroscopy and Reddy et al.<sup>21</sup> using <sup>13</sup>C NMR all confirmed that lithium ions are almost exclusively solvated by cyclic carbonates in electrolyte solutions with mixed linear and cyclic carbonates. Thus, it is not surprising to find that the

SEI formed in this electrolyte would be dictated by EC reduction rather than EMC reduction.

Finally, we feel it is important to discuss the physical structure of the lithium ethylene dicarbonate layer, although we have no direct evidence of what this structure is. Our FTIR spectrum of the synthetic compound and the quantum chemical calculations (Hartree-Fock) used to interpret the spectrum indicate that intermolecular association through O...Li...O interactions is very important in this compound. Wang and Balbuena<sup>12</sup> have conducted a detailed quantum chemical (B3PW91) study of the O...Li...O interactions and resulting intermolecular conformations in a number of lithium alkyl dicarbonates, including the dicarbonate of interest here. They concluded that the linear *n*-mer chainlike structure, the dimer of which we used here, is not as energetically favorable as a three-dimensional cage-like network structure, which has a higher Li...O coordination than the linear chains. However, the IR spectrum they calculate for more highly Li...O coordinated structures, relative to those calculated for the dimer/trimer/tetramer structures, introduces frequency shifts and additional peaks that we did not see in our experimental spectrum *n*-mer. Therefore, it appears from data available at present that the (CH<sub>2</sub>OCO<sub>2</sub>Li)<sub>2</sub> layer has a highly associated structure from relatively strong O...Li...O interactions and that this associated structure plays an important role in the passivating nature of the layer. The exact intermolecular conformation of the (CH<sub>2</sub>OCO<sub>2</sub>Li)<sub>2</sub> is, however, not yet established.

## V. Conclusions

By comparison of IR experimental spectra with that of the synthesized compound, we established that (CH<sub>2</sub>OCO<sub>2</sub>Li)<sub>2</sub> is the predominant surface species on a Ni electrode after lithium deposition in LiPF<sub>6</sub>/EC:EMC (3:7) electrolyte. We also found that lithium ethylene dicarbonate is the passivation layer that forms on metallic lithium cleaved in situ in the same electrolyte. Detailed analysis of the IR spectrum utilizing quantum chemical calculations (Hartree-Fock) indicates that intermolecular association through O...Li...O interactions is very important in this compound. It is likely that the (CH<sub>2</sub>OCO<sub>2</sub>Li)<sub>2</sub> passivation layer has a highly associated structure, but the exact intermolecular conformation of the (CH<sub>2</sub>OCO<sub>2</sub>Li)<sub>2</sub> could not be established on the basis of analysis of the IR spectrum.

**Acknowledgment.** This work was supported by the Office of Advanced Automotive Technologies and the Office of FreedomCAR and Vehicle Technologies, of the U.S. Department of Energy under Contract Nos. DE-AC03-76SF00098 (LBNL) and DE-AI01-99EE5061 (ARL), respectively.

## References and Notes

- (1) Aurbach, D.; Daroux, M. L.; Faguy, P. W.; Yeager, E. J. *Electrochem. Soc.* **1987**, *134*, 1611.
- (2) Aurbach, D.; Gofer, Y.; Ben-Zion, M.; Aped, P. J. *Electroanal. Chem.* **1992**, *339*, 451.
- (3) Aurbach, D.; Ein-Ely, Y.; Zaban, A. *Electrochem. Soc. Lett.* **1994**, *141*, L1.
- (4) Aurbach, D.; Ein-Ely, Y.; Chusid, O.; Carmeli, Y.; Babai, M.; Yamin, H. J. *Electrochem. Soc.* **1994**, *141*, 603.
- (5) Aurbach, D.; Ein-Ely, Y.; Markovsky, B.; Zban, A.; Luski, S.; Carmeli, Y.; Yamin, H. J. *Electrochem. Soc.* **1995**, *142*, 2882.
- (6) Xu, K. *Chem. Rev.* **2004**, *104*, 4303.
- (7) Gireaud, L.; Grugeon, S.; Laruelle, S.; Pilard, S.; Tarascon, J.-M. *J. Electrochem. Soc.* **2005**, *152*, A850.
- (8) Zhuang, G. V.; Ross, P. N. *Electrochem. Solid-State Lett.* **2003**, *6*, A136.
- (9) Song, S.-W.; Zhuang, G. V.; Ross, P. N. *J. Electrochem. Soc.* **2004**, *151*, A1162.

- (10) Frisch, M. J.; Trucks, G. W.; Schlegel, H. B.; Scuseria, G. E.; Robb, M. A.; Cheeseman, J. R.; Zakrzewski, V. G.; Montgomery, J. A.; Stratmann, R. E.; Burant, J. C.; Dapprich, S.; Millam, J. M.; Daniels, A. D.; Kudin, K. N.; Strain, O. F. M. C.; Tomasi, J.; Barone, B.; Cossi, M.; Cammi, R.; Mennucci, B.; Pomelli, C.; Adamo, C.; Clifford, S.; Ochterski, J.; Petersson, G. A.; Ayala, P. Y.; Cui, Q.; Morokuma, K.; Malick, D. K.; Rabuck, A. D.; Raghavachari, K.; Foresman, J. B.; Ciolovski, J.; Ortiz, J. V.; Stefanov, V. V.; Liu, G.; Liashenko, A.; Piskorz, P.; Komaromi, I.; Gomperts, R.; Martin, R. L.; Fox, D. J.; Keith, T.; Al-Laham, M. A.; Peng, C. Y.; Nanayakkara, A.; Gonzalez, C.; Challacombe, M.; Gill, P. M. W.; Johnson, B.; Chen, W.; Wong, M. W.; Andres, J. L.; Head-Gordon, M.; Replogle, E. S.; Pople, J. A. *Gaussian 98*, revision A.11.3; Gaussian, Inc.: Pittsburgh, PA, 1998.
- (11) Pople, J. A.; Krishnan, R.; Schlegel, H.; Binkley, J. S. *Int. J. Quantum Chem. Symp.* **1979**, 13, 225.
- (12) Wang Y.; Balbuena, P. B. *J. Phys. Chem. A* **2002**, 106, 9582.
- (13) Staikov, G.; Lorenz, W. J.; Budevski, E. Low-Dimensional Metal Phases and Nanostructuring of Solid Surfaces. In *Imaging of Surface and Interfaces*; Lipskowsky, J., Ross, P. N., Eds.; Wiley-VCH: New York, 1999; Chapter 1.
- (14) (a) Pletcher, D.; Rohan, J.; Ritchie, A. *Electrochim Acta* **1994**, 39, 1369. (b) Pletcher, D.; Rohan, J.; Ritchie, A. *Electrochim Acta* **1994**, 39, 2015.
- (15) Ota, H.; Shima, K.; Ue, M.; Yamaki, J. *Electrochim Acta* **2004**, 49, 565.
- (16) Jeong, S.-K.; Inaba, M.; Abe T.; Ogumi, Z. *J. Electrochem. Soc.* **2001**, 148, A989.
- (17) Zhang, X.; Kostecki, R.; Richardson, T. J.; Pugh J. K.; Ross, P. N. *J. Electrochem. Soc.* **2001**, 148, A1341.
- (18) Wang, Y.; Nakamura, S.; Ue, M.; Balbuena, P. B. *J. Am. Chem. Soc.* **2001**, 123, 11708.
- (19) Wang, Y.; Balbuena, P. B. *Int. J. Quantum Chem.* **2005**, 102, 724.
- (20) (a) Fukushima, T.; Matsuda, Y.; Hashimoto, H.; Arakawa, R. *Electrochem. Solid-State Lett.* **2001**, 4, A127. (b) Matsuda, Y.; Fukushima, T.; Hashimoto, H.; Arakawa, R. *J. Electrochem. Soc.* **2002**, 149, A1045.
- (21) Reddy, V. P.; Smart, M. C.; Chin, K. B.; Ratnakumar, B. V.; Surampudi, S.; Hu, J.; Yan, P.; Prakash, G. K. S. *Electrochem. Solid-State Lett.* **2005**, 8, A294.